Title: Effect of Solution Heat Treatment on Microstructure and Mechanical Properties of Laser Powder Bed Fusion produced Cobalt-28Chromium-6Molybdenum

Authors:

Swee Leong Sing, (S.L. Sing) sing0011@e.ntu.edu.sg

Sheng Huang (S. Huang) sheng007@e.ntu.edu.sg

Wai Yee Yeong, (W.Y. Yeong) wyyeong@ntu.edu.sg +65 6790 4343 (corresponding author)

Affiliations:

Singapore Centre for 3D Printing, School of Mechanical & Aerospace Engineering, Nanyang Technological University

Address: N3.1-B2C-03, 50 Nanyang Avenue, Singapore 639798

Keywords: Additive Manufacturing, 3D Printing, Selective Laser Melting, Powder Bed Fusion, Heat Treatment

Abstract:

Cobalt-chromium-molybdenum (CoCrMo) alloys have excellent properties that make them widely used in dental applications. Selective laser melting (SLM) is a laser powder bed fusion (L-PBF) additive manufacturing, or 3D printing, technique that can fabricate functional parts directly using these alloys.

In this work, SLM is used to fabricate CoCrMo samples and they underwent different heat treatment originally designed for casted CoCrMo alloy. The mechanical properties, such as ultimate tensile strength, yield strength and microhardness of the heat treated SLM CoCrMo parts are evaluated and benchmarked against their casted counterparts. It is found that as-built samples have anisotropy properties while heat treated samples displayed isotropic properties. As-built SLM CoCrMo specimens demonstrated approximately twice the yield strength (YS) and ultimate tensile strength (UTS) as compared to ASTM F75 standard for cast CoCrMo alloys. However, both UTS and YS of SLM CoCrMo decreased after heat treatment. The microstructure analysis concluded carbides formation because of heat treatment.

1. Introduction

Cobalt-chromium-molybdenum (CoCrMo) alloys have excellent corrosion resistance, biocompatibility and strength [1]. As such, they have been widely used in dental applications, such as removable partial dentures, metal frames, customized abutments, crowns and bridges in the anterior and posterior regions [2, 3]. Selective laser melting (SLM) is a laser powder bed fusion (L-PBF) additive manufacturing [4], also commonly known as 3D printing, technique that uses a laser power source to fuse powder materials to form functional parts directly based on

computer aided design (CAD) file. The details of the SLM process have been described in various works [5-7].

The capability of SLM to produce customizable products has led to extensive research of using this process for applications in the biomedical field [8-10]. Several works have been reported on the production of CoCrMo alloys using SLM for various implants [2, 3, 11-13]. A. Takaichi *et al.* investigated the mechanical properties and metal elution of CoCrMo alloy fabricated by SLM. It is reported that the as-built SLM parts have yield strength, ultimate tensile strength and elongation that were high than those of the as-cast alloy and satisfied the type 5 criteria in ISO 22764. Furthermore, the metal elution from the SLM built parts was lesser than that of the as-cast alloy [3]. S. Yager *et al.* manufactured CoCrMo partially removable denture clasps using SLM. It is shown that SLM CoCrMo clasps have similar mechanical properties compared to clasps formed by conventional lost-wax casting [13]. Caravaggi *et al.* fabricated porous CoCrMo scaffolds using SLM, and investigated their topographical, mechanical and biological properties for orthopedic applications. While geometrical inaccruracies were found in the samples compared to the designs, it is concluded that they show similar *in vitro* biological activity, mechanical properties that are sutiable for orthopedic applications [14].

Despite the prior research done, there is still limited information on the effect of post-process heat treatment on SLM CoCrMo alloys [15, 16]. While studies have been conducted on heat treat on SLM heat treatment, there is no study conducted on the effect of solution heat treatment duration on this material [17, 18]. This research is of great interest due to the difference in SLM CoCrMo microstructure compared to same alloy formed by conventional methods [13, 19]. In this paper, CoCrMo alloy is fabricated using selective laser melting and underwent different heat treatment originally designed for casted CoCrMo alloy. The microstructure, and mechanical

properties of heat treated SLM produced CoCrMo parts are reported. The mechanical properties, such as ultimate tensile strength, yield strength and microhardness of the heat treated SLM CoCrMo parts are evaluated and benchmarked against their casted counterparts.

2. Experimental details

2.1. Material

The samples were fabricated using CoCrMo (ASTM F75, Apphia Advanced Materials Pte Ltd, Singapore) gas atomized powder with particle size distribution of 20 to 63 μm. The scanning electron microscopy (SEM) image of the powder is shown in Fig. 1, in which spherical powder particles with some satellites are observed.

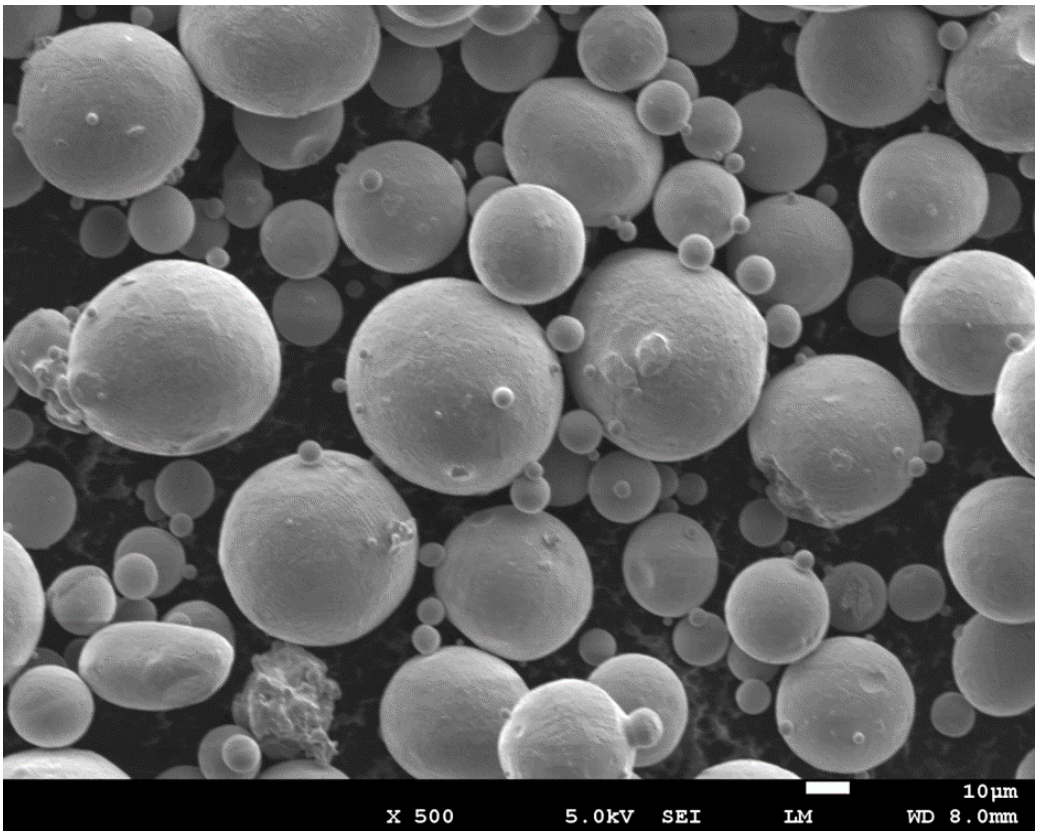

Fig. 1. SEM image of CoCrMo powder.

The spherical powder particles is essential for good flowability, which is needed for uniform powder deposition during SLM [20, 21]. The composition of the powder was determined by inductively coupled plasma atomic emission spectroscopy (ICP-AES) and tabulated in Table 1.

Table 1 Composition of CoCrMo powder

Alloying elements	**ASTM F75 (wt%)**	**ICP-AES (wt%)**
Chromium	27 – 30	27
Molybdenum	5 – 7	7
Nickel	< 0.5	0.063
Iron	< 0.75	0.00
Carbon	< 0.35	0.001
Silicon	< 1	0.6
Manganese	< 1	0.5
Tungsten	< 0.2	0.15
Phosphorus	< 0.02	0.001
Sulphur	< 0.01	0.005
Nitrogen	< 0.25	0.1
Aluminum	< 0.1	0.001
Titanium	< 0.1	0.005
Boron	< 0.01	0.001
Cobalt	Balance	Balance

2.2. Selective laser melting

Fabrication of all the samples was carried out on a SLM 250HL machine (SLM Solutions Group AG, Germany). The SLM machine is equipped with a Gaussian beam fiber laser with maximum power of 400 W and a focal diameter of 80 μm. All processing occurred in an argon environment with less than 0.05 % oxygen to prevent oxidation and degradation of the material during the process. Sectorial, also known as island or chessboard, scanning was used to minimize thermal stresses formed during the process. The process parameters are shown in Table 2. The parameters were chosen as this combination can produce parts that are of full density, as determined by Archimedes' Principle.

Table 2 SLM processing parameters for CoCrMo

Process parameters	
Laser power (W)	360
Laser scan speed (mm/s)	500
Layer thickness (μm)	50
Hatch spacing (mm)	0.175
Remelting	No
Island length (mm)	5 x 5
Island overlap (mm)	1
Substrate heating (^{o}C)	100
Relative density (%)	99.9

2.3. Heat treatment

The heat treatment cycles were designed based on results obtained by previous research, which provided maximum improvement in mechanical properties of cast CoCrMo alloys [22, 23]. The heat treatment cycles are summarized in Table 3. Rapid quenching in water at room temperature was done at the end of preheating and solution treatment. The heat treatment was done using a laboratory chamber furnace (Elite Thermal Systems Limited).

Table 3 Designed heat treatment cycles for CoCrMo

Heat treatment	**Duration (hours)**		
	A	**B**	**C**
Preheating (815 ^{o}C)		4	
Solution treatment (1220 ^{o}C)	1	2	4

2.4. Metallographic characterization

The samples were subjected to standard metallographic procedure. Metallographic samples' preparation was carried out with a Struer's Tagamin 25. #320 silicon carbide papers were first used to grind the surface of SLM as-built and heat treated CoCrMo samples. Struer's MD-Largo disc was then employed with Allegro/Largo 9 μm suspension. It was followed by MD-Dac disc accompanied by Dac 3 μm suspension. The final polishing was conducted using an MD-Chem disc with OP-S active oxide polishing suspension. The samples were then etched by immersion in 36 % hydrochloric acid for ~8 hours [1, 2]. The microstructure study was conducted using optical microscopy (OM, Zeiss), scanning electron microscopy (SEM, JEOL JSM7600) and X-

ray diffraction (XRD, Empyrean from Panalytical). Grain size measurements of the samples were done using image analysis with ImageJ from images obtained by OM.

2.5. Mechanical characterization

Tensile coupons, based on ASTM E8, were produced using wire-cut discharge machining (EDM) from blocks fabricated by SLM. An Instron Static Tester Series 5569, 50 kN machine was used and a loading speed of 1 mm/min was applied on all tensile samples. Tensile test loading direction was perpendicular to the build direction of the samples.

The microhardness test of the material was carried out using FM-300e Vickers hardness machine on the xy- and yz- planes where a load of 1 kg and a loading time of 15 s were used.

All average values and standard deviations are calculated from five data points from different samples.

3. Results and discussion

3.1. Microstructure

Based on the processing parameters chosen, the as-built specimens from SLM exhibit heterogeneous microstructure under OM observations, as shown in Fig. 2(a) and Fig. 2(b).

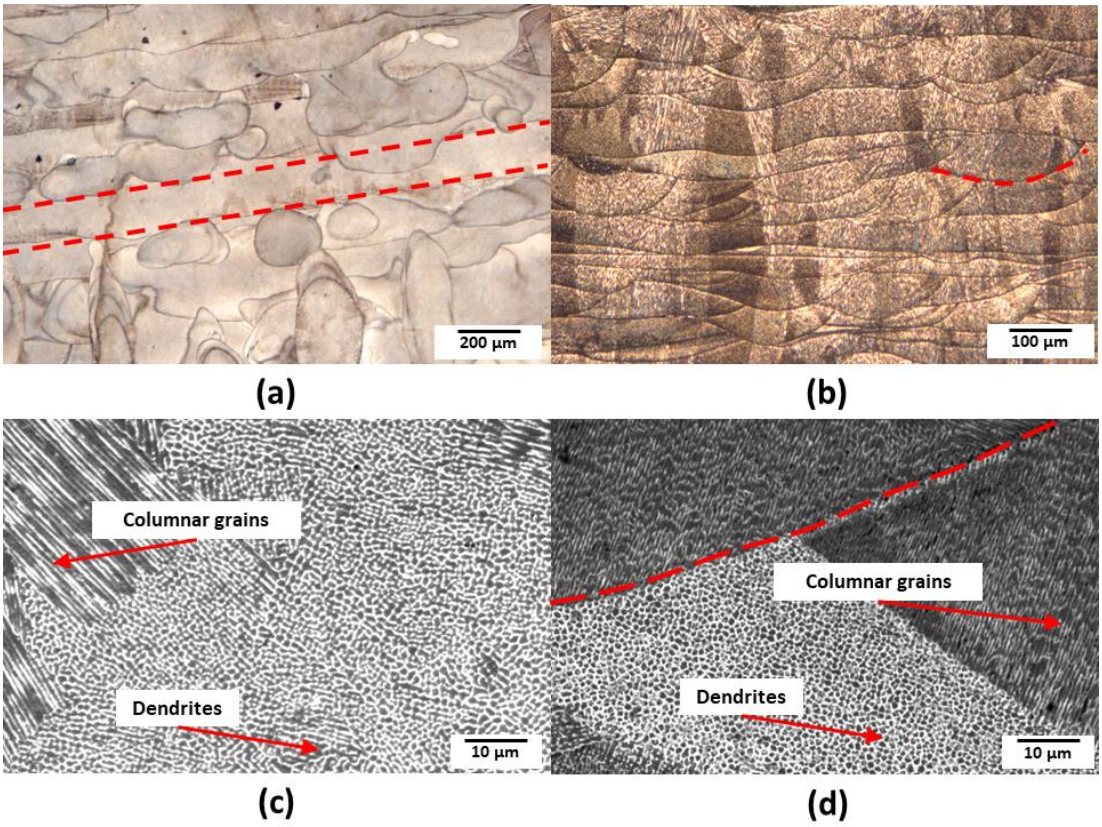

Fig. 2. OM images in (a) xy-plane (b) yz-plane and SEM images in (c) xy-plane (d) yz-plane of as-built SLM CoCrMo alloys specimens. The red dotted lines indicate the melt pool boundary.

The rapid solidification of adjacent scan tracks revealed a network of overlapping melt pools in the xy-plane (Fig. 2 (a)) and half cylinder melt pools boundaries in the yz-plane (Fig. 2 (b)), which is the typical characteristic of as-built SLM samples. The physical phenomena that occur during SLM is very similar to those observed in welding process [24]. Melt pools are formed when the laser irradiates the powder bed and becomes elongated when the laser moves. The melt pool shape then changes from round or slightly elliptical to teardrop under the induced heat flow. The shapes observed in Fig. 2(b), seen as ripple solidification, were formed by the sequential solidification of teardrop melt pools. In addition, fine lamellae elongated along the build direction can be observed, as shown in Fig. 2(b). During the SLM, the crystalline grains in the

previous layers acted as nucleation sites for further solidification of melt through heterogeneous nucleation, yielding the formation of the vertical columnar grains. Under SEM, the as-built specimens consist of fine cellular and elongated dendritic microstructure features, shown in Fig. 2(c) and Fig. 2(d). During welding, the direction of maximum temperature gradient is always perpendicular to the melt pool boundary, however, in SLM, the formed melt pool was surrounded by loose powder that negatively affect the heat flow. A competitive growth during the dendrite formations can occur which can result in different growth directions. Due to the high thermal gradient and the rapid solidification rate which were involved in the SLM processing, fine columnar or cellular microstructure would also be formed [2]. In particular, fine γ-Co columnar grains consisting of dendrites were formed due to the dendritic segregation of Cr and Mo elements [25].

The microstructure of heat-treated specimens are shown in Fig. 3.

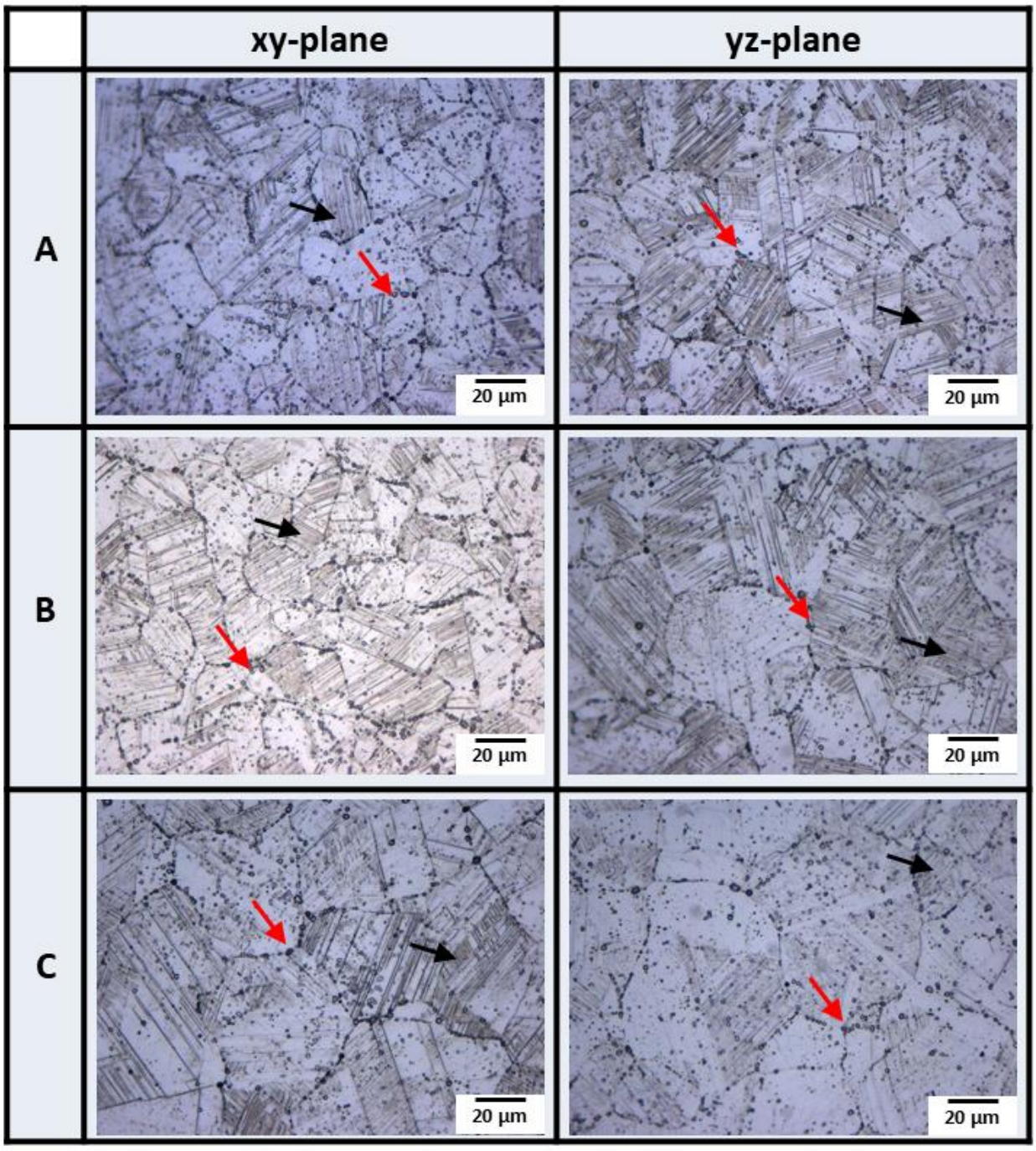

Fig. 3. OM images for heat treated specimens.

The microstructure of heat-treated specimens showed that recrystallization of the grains have occurred since no traces, such as melt tracks and melt pools, of the SLM process were observed. No differences in microstructure were observed in the xy- and yz-planes under each heat

treatment conditions. Large equiaxed grains were also observed compared to the cellular grains present in the as-built SLM specimens.

The heat-treated specimens showed similar features regardless of their solution heat treatment duration. The carbides, observed as spherical spots in the microstructures, as indicated by the red arrows in Fig. 3, are consistent with those formed in CoCrMo processed by laser engineered net shaping (LENS), a directed energy deposition AM technique [26]. Formation of heavily faulted phases within each grain were observed, indicated by black arrows in Fig. 3. These phases exhibit "plate-like" structures, like martensite in steels. These "plate-like" appearances corresponds to the nucleation of HCP phases at the intersections of FCC [27]. While the heat-treated specimens showed similar features, the solution heat treatment duration has effect on the grain size. While there is no significant change in grain size between samples in Group A and B, at 4 hours solution heat treatment, there is observable increased in grain size (Group C), as shown in Table 4.

Table 4 Grain Size of CoCrMo after solution heat treatment

	xy-plane (µm)	**yz-plane (µm)**
A	40.45 ± 9.49	30.71 ± 6.61
B	40.52 ± 6.83	38.03 ± 10.75
C	50.85 ± 18.44	54.38 ± 20.09

The nucleation of martensite and formation of carbides are commonly observed in CoCrMo alloys. The amount of carbides formed along the grain boundaries were significantly higher in

specimens which had undergone 2 hours and 4 hours of solution heat treatment as compared to those for 1 hour. It has been reported that amount of carbides increased with aging time, but can decrease with solution heat treatment duration [15, 18]. Therefore, the preheating may result in precipitation of carbides along the grain boundaries and matrix, however, the increase in solution heat treatment duration may cause a decrease in amount of carbides [28]. The formation of carbides after heat treatment is confirmed using XRD, as shown in Fig. 4. Unidentified peaks are also observed in previous studies [18].

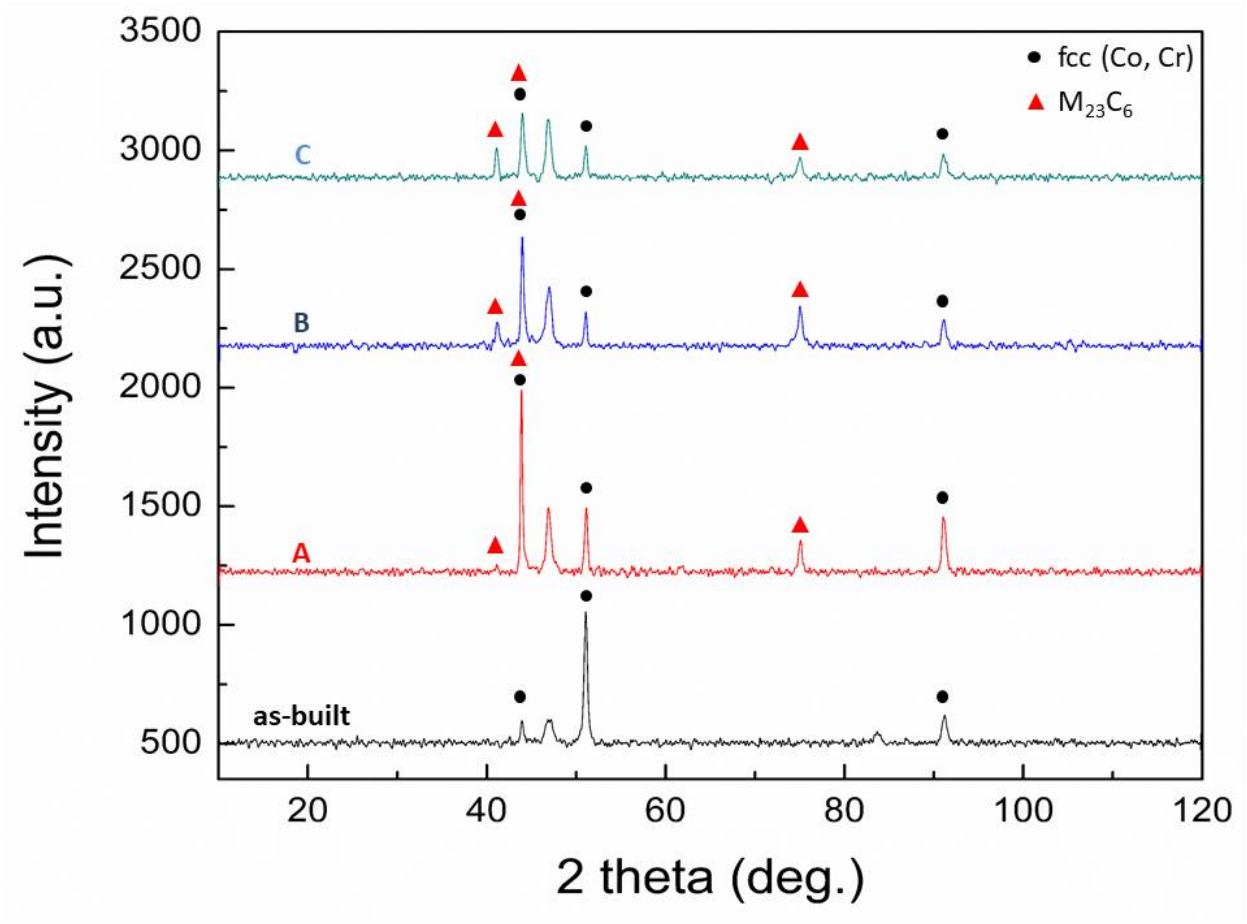

Fig. 4. XRD spectrums of SLM as-built CoCrMo, 1 hour solution heat treated (A), 2 hours solution heat treated (B) and 4 hours solution heat treated (C) specimens.

It can be seen from Fig. 4, the as-built samples do not have any carbides precipitates. At heat treatment temperature of 1220 °C, increasing the holding time allow more diffusion and more carbides can dissolve in the matrix and therefore the concentration of precipitates decreased in CoCrMo alloy with increased solution heat treatment duration [29]. This is evident by the decrease in intensity of the peaks in the XRD patterns for the carbides as the solution heat treatment duration increases.

3.2. Mechanical properties

The micro-hardness in the xy-plane and yz-plane of the specimens are shown in Fig.5. The xy-plane and yz-plane represents the planes perpendicular and parallel to the build direction respectively. The values for the cast samples are obtained from previous study [30].

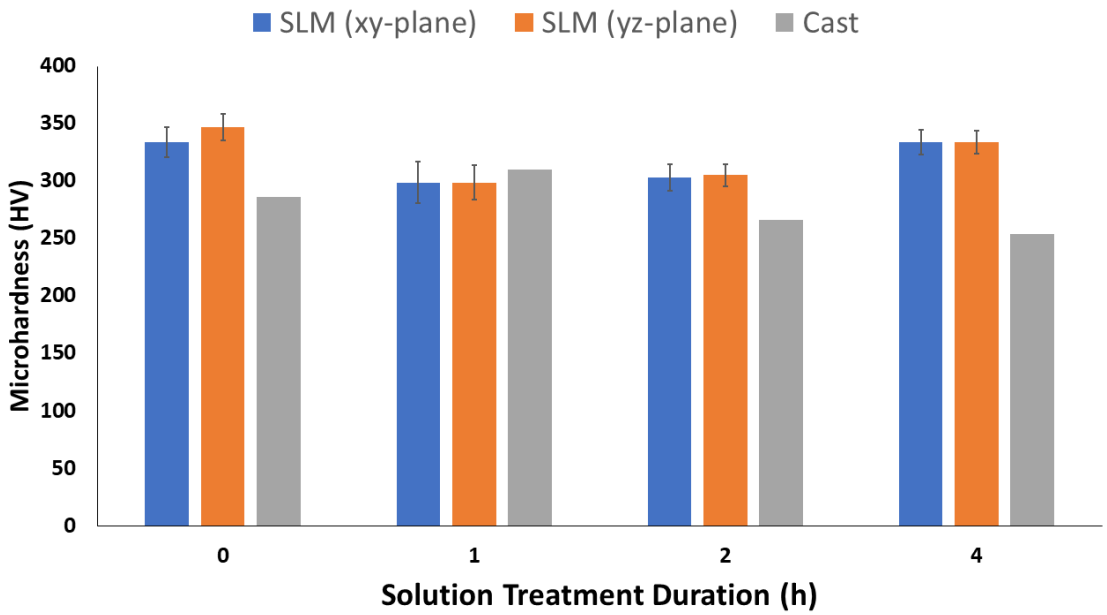

Fig. 5. Micro-hardness of CoCrMo fabricated by SLM and casting.

As-built SLM specimens demonstrated higher micro-hardness values in the yz-planes as compared to the xy-planes which is observed in other SLM parts [67]. On the other hand, all

heat-treated specimens showed similar micro-hardness values in both xy- and yz-planes. This was attributed by recrystallization that may have occurred during the heat treatment process which resulted in reduction in mechanical anisotropy in the SLM parts [68]. The micro-hardness after 1 hour solution heat treatment was reduced significantly by approximately 10 %, and increased after the first hour. The initial decrease in microhardness after 1 hour solution heat treatment in the SLM samples can be attributed to the stress relief effect from the heat treatment [15]. The increase in microhardness after 1 hour solution heat treatment can be attributed to formation of the carbides which outweighs the stress relief effect. The results showed an opposite trend as compared to the cast ASTM F75 CoCrMo alloys, whereby the micro-hardness decreased from 1 hour to 4 hours of solution treatment due to the dissolution of the carbides into the matrix.

The tensile properties of the specimens before and after heat treatment, in comparison with ASTM F75 requirements for cast CoCrMo alloys, are shown in Fig. 6.

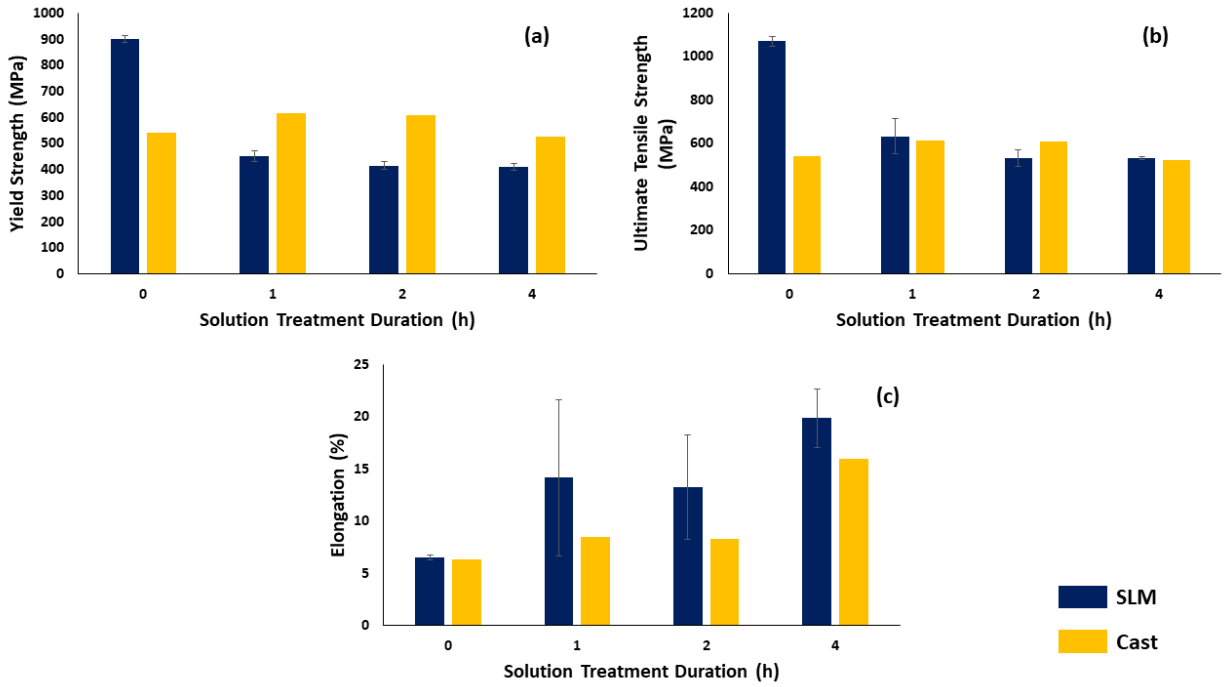

Fig. 6. Tensile properties of CoCrMo fabricated by SLM and casting (a) yield strength (b) ultimate tensile strength (c) elongation.

As-built SLM specimens demonstrated approximately twice the values in YS and UTS, as compared to ASTM F75 standard for cast CoCrMo alloys. The results confirm that CoCrMo alloys manufactured using SLM have tensile properties that are superior to cast CoCrMo alloys. However, upon preheating and 1 hour solution heat treatment, both UTS and YS of CoCrMo were reduced drastically by 50.0 % and 40.9 % respectively. The strengths decreased gradually as the solution heat treatment time was increased to 2 hours and stabilized at 4 hours solution treatment time. However, from the results obtained for cast CoCrMo, YS and UTS were showed to, first, increase upon 1 hour solution heat treatment before gradually decreasing as the duration increases [30]. The microstructure analysis concluded carbides formation because of heat treatment. Carbides formation along the grain boundaries are similar in SLM specimens and cast specimens, which attributed to the reduction in strength but increase in ductility. Furthermore, lower tensile strength from the heat-treated specimens can be due to the relative larger grains observed compared to those in as-built specimens. The plate-like martensitic phases formed after heat treatment also contributes to stress concentrations which significantly reduces the UTS and YS of the specimens [30]. In addition, it is known that the presence of carbides at the grain boundaries and inside the grains can promote alloy strengthening. The carbides at the grain boundaries prevent them from sliding and migrating while carbides inside the grains strengthen the alloy matrix by providing obstacles to dislocations [17].

The classic Hall–Petch formula states that fine grains alleviate the deformation differences between intra-granular and grain boundaries (the bamboo joint phenomenon), leading to greater capacity for homogeneous coordination. Strengths were enhanced, because crackle propagation

was rendered difficult due to obstruction of the grain boundaries. Prior to heat treatments, the SLM CoCrMo has higher strength as compared to the cast counterparts. This is principally due to the grain size at the submicron level. The total length of grain boundary increased dramatically, and the numbers of internal dislocations reduced substantially. Meanwhile, deformation was no longer heavily dependent on the crystal dislocation mechanism, and grain boundary movement became more important. In this case, the microcosmic mechanisms (e.g. crystal boundary migration, grain rotation, and shearing localization) played a substantial role.

Following heat treatment, SLM samples provided lower UTS and YS but higher elongation, as compared to cast CoCrMo. This implies that the material failure mechanism started to change from brittle to ductile fracture, resulting in greater elongation. The grains began to grow in size after heat treatment, and deformation occurred through the crystal dislocation mechanism rather than the crystal boundary movement mechanism. Elongation increased while yield strength decreased [16]. This was verified by the amplified morphology of the fracture of the SLM fabricated parts before and after heat treatment, as shown in Fig. 7.

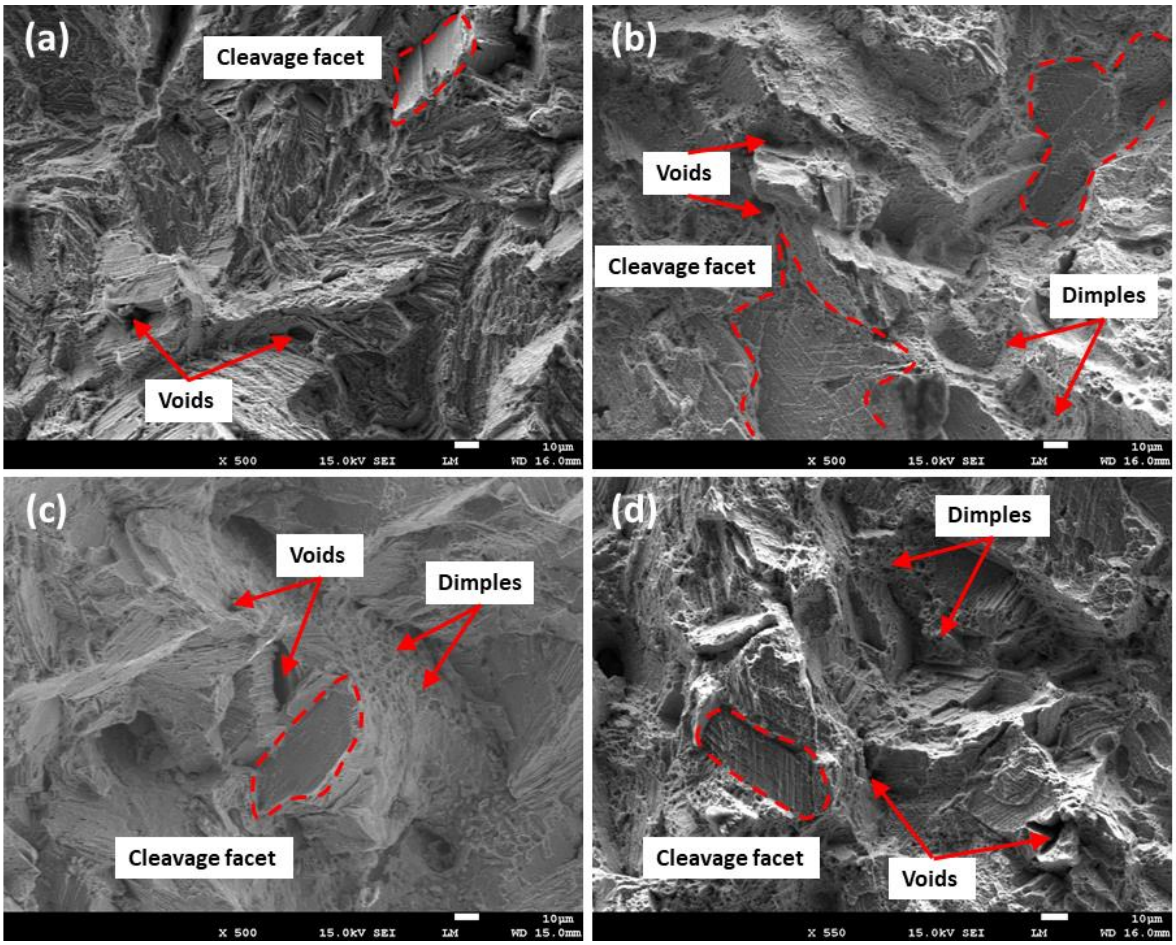

Fig. 7. Fracture surfaces of (a) as-built (b) A (c) B and (d) D specimens.

The as-built specimens exhibit fractures that are predominantly brittle. In general, brittle fracture propagates through the grains, and produce a terrace-like steps when crossing grain boundaries. Furthermore, the newly created crack planes join during further propagation, forming river-like pattern. During SLM, the grains solidified quickly before they can grow substantially in size. Usually, the smaller the grains size, the greater the number of grain boundaries which results in greater resistance in dislocation. This leads to higher UTS and YS. At microscopic level, ductile fractures are characterized by dimples which arises from cavities formed from coarser precipitates, which in this case, are from the carbides. The carbides are absent from the as-built specimens, which explains the lack of dimples. This demonstrates that after heat treatment, the

fracture mechanism changed from brittle to ductile. The cleavages are formed by separation along a well-defined crystallographic plane. The flatness of the cleavage facets suggests the idea that only two atomic planes forming the fracture surfaces are involved in the crack process. In contrast, the heat treated specimens exhibit a mixture of ductile and brittle fracture, as characterized by the presence of dimples, voids and cleavages. The fractures were proceeded predominantly by ductile intragranular fracture mode with dimple-like morphology.

4. Conclusions

In this paper, CoCrMo alloy is fabricated using selective laser melting and underwent different heat treatment originally designed for casted CoCrMo alloy. The microstructure, and mechanical properties of heat treated SLM produced CoCrMo parts are reported. The mechanical properties, such as ultimate tensile strength, yield strength and microhardness of the heat treated SLM CoCrMo parts are evaluated and benchmarked against their casted counterparts.

The key findings of this research include:

1) As-built SLM CoCrMo specimens have anisotropy properties. They displayed higher micro-hardness values in the yz-planes as compared to the xy-planes. On the other hand, all heat treated specimens showed similar micro-hardness values in both xy- and yz-planes.

2) As-built SLM CoCrMo specimens demonstrated approximately twice the values in YS and UTS, as compared to ASTM F75 standard for cast CoCrMo alloys.

3) After heat treatment, both ultimate tensile strength and yield strength of SLM CoCrMo decreased. The strengths decreased gradually as the solution heat treatment time was

increased to 2 hours and stabilized at 4 hours solution treatment time. The microstructure analysis concluded carbides formation because of heat treatment.

DATA AVAILABILITY

The raw/processed data required to reproduce these findings cannot be shared at this time due to technical or time limitations

REFERENCES

[1] B. Qian, K. Saeidi, L. Kvetková, F. Lofaj, C. Xiao, Z. Shen, Defects-tolerant Co-Cr-Mo dental alloys prepared by selective laser melting, Dental Materials 31 (2015) 1435-1444.

[2] Y.S. Hedberg, B. Qian, Z. Shen, S. Virtanen, I.O. Wallinder, In vitro biocompatibility of CoCrMo dental alloys fabricated by selective laser melting, Dental Materials 30 (2014) 525-534.

[3] A. Takaichi, Suyalatu, T. Nakamoto, N. Joko, N. Nomura, Y. Tsutsumi, S. Migita, H. Doi, S. Kurosu, A. Chiba, N. Wakabayashi, Y. Igarashi, T. Hanawa, Microstructure and mechanical properties of Co-29Cr-6Mo alloy fabricated by selective laser melting process for dental applications, Journal of the Mechanical Behavior of Biomedical Materials 21 (2013) 67-76.

[4] A.M. Khorasani, I. Gibson, A. Ghasemi, A. Ghaderi, A comprehensive study on variability of relative density in selective laser melting of Ti-6Al-4V, Virtual and Physical Prototyping 14(4) (2019) 349-359.

[5] S.L. Sing, S. Wang, S. Agarwala, F.E. Wiria, T.M.H. Ha, W.Y. Yeong, Fabrication of titanium based biphasic scaffold using selective laser melting and collagen immersion, International Journal of Bioprinting 3(1) (2017) 65-71.

[6] A. Salmi, E. Atzeni, History of residual stresses during the production phases of AlSi10Mg parts processed by powder bed additive manufacturing technology, Virtual and Physical Prototyping 12(2) (2017) 153-160.

[7] R. Martinez, I. Todd, K. Mumtaz, In situ alloying of elemental Al-Cu12 feedstock using selective laser melting, Virtual and Physical Prototyping 14(3) (2019) 242-252.

[8] S.L. Sing, F.E. Wiria, W.Y. Yeong, Selective laser melting of lattice structures: A statistical approach to manufacturability and mechanical behavior, Robotics and Computer-Integrated Manufacturing 49 (2018) 170-180.

[9] S.L. Sing, W.Y. Yeong, F.E. Wiria, B.Y. Tay, Z. Zhao, L. Zhao, Z. Tian, S. Yang, Direct selective laser sintering and melting of ceramics: a review, Rapid Prototyping Journal 23(3) (2017) 611-623.

[10] T. Long, X. Zhang, Q. Huang, L. Liu, J. Ren, Y. Yin, D. Wu, H. Wu, Novel Mg-based alloys by selective laser melting for biomedical applications: microstructure evolution, microhardness and in vitro degradation behaviour, Virtual and Physical Prototyping 13(2) (2018) 71-81.

[11] E. Liverani, A. Fortunato, A. Leardini, C. Belvedere, S. Siegler, L. Ceschini, A. Ascari, Fabrication of Co-Cr-Mo endoprosthetic ankle devices by means of Selective Laser Melting (SLM), Materials and Design 106 (2016) 60-68.

[12] C. Song, Y. Yang, Y. Wang, J.-k. Yu, D. Wang, Personalized femoral component design and its direct manufacturing by selective laser melting, Rapid Protoyping Journal 22(2) (2016) 330-337.

[13] S. Yager, J. Ma, H. Ozcan, H.I. Kilinc, A.H. Elwany, I. Karaman, Mechanical properties and microstructure of removable partial denture clasps manufactured using selective laser melting, Additive Manufacturing 8 (2015) 117-123.

[14] P. Caravaggi, E. Liverani, A. Leardini, A. Fortunato, C. Belvedere, F. Baruffaldi, M. Fini, A. Parrilli, M. Mattioli-Belmonte, L. Tomesani, S. Pagani, CoCr porous scaffolds manufactured via selective laser melting in orthopedics: Topographical, mechanical, and biological characterization, Journal of Biomedial Materials Research: Part B Applied Biomaterials (2019).

[15] M. Zhang, Y. Yang, C. Song, Y. Bai, Z. Xiao, An investigation into the aging behavior of CoCrMo alloys fabricated by selective laser melting, Journal of Alloys and Compounds 750 (2018) 878-886.

[16] C. Song, M. Zhang, Y. Yang, D. Wang, J.-k. Yu, Morphology and properties of CoCrMo parts fabricated by selective laser melting, Materials Science and Engineering: A 713 (2018) 206-213.

[17] Y. Kajima, A. Takaichi, N. Kittikundecha, T. Nakamoto, T. Kimura, N. Nomura, A. Kawasaki, T. Hanawa, H. Takahashi, N. Wakabayashi, Effect of heat-treatment temperature on microstructures and mechanical properties of Co–Cr–Mo alloys fabricated by selective laser meltin, Materials Science and Engineering: A 726 (2018) 21-31.

[18] K.K. Bawane, D. Srinivasan, D. Banerjee, Microstructural Evolution and Mechanical Properties of Direct Metal Laser-Sintered (DMLS) CoCrMo After Heat Treatment, Metallurgical and Materials Transactions A 49(9) (2018) 3793-3811.

[19] Y.S. Al Jabbari, T. Koutsoukis, X. Barmagadaki, S. Zinelis, Metallurgical and interfacial characterization of PFM Co-Cr dental alloys fabricated via casting, milling or selective laser melting, Dental Materials 30(4) (2014) e79-e88.

[20] S.L. Sing, W.Y. Yeong, F.E. Wiria, Selective laser melting of titanium alloy with 50 wt% tantalum: Microstructure and mechanical properties, Journal of Alloys and Compounds 660 (2016) 461-470.

[21] A.T. Sutton, C.S. Kriewall, M.C. Leu, J.W. Newkirk, Powder characterisation techniques and effects of powder characteristics on part properties in powder-bed fusion processes, Virtual and Physical Prototyping 12(1) (2017) 3-29.

[22] C. Montero-Ocampo, H. Lopez, M. Talavera, Effect of alloy preheating on the mechanical properties of as-cast Co-Cr-Mo-C alloys, Metallurgical and Materials Transactions A 30(3) (1999) 611-620.

[23] Y. Bedolla-Gil, M.A.L. Hernandez-Rodriguez, Tribological Behavior of a Heat-Treated Cobalt-Based Alloy, Journal of Materials Engineering and Performance 22(2) (2013) 541-547.

[24] X. Zhou, K. Li, D. Zhang, X. Liu, J. Ma, W. Liu, Z. Shen, Textures formed in a CoCrMo alloy by selective laser melting, Journal of Alloys and Compounds 631 (2015) 153-164.

[25] D.D. Xiang, P. Wang, X.P. Tan, S. Chandra, C. Wang, M.L.S. Nai, S.B. Tor, W.Q. Liu, E. Liu, Anisotropic microstructure and mechanical properties of additively manufactured Co–Cr–Mo alloy using selective electron beam melting for orthopedic implants, Materials Science and Engineering: A (2019).

[26] G.D. Janaki Ram, C.K. Esplin, B.E. Stucker, Microstructure and wear properties of LENS® deposited medical grade CoCrMo, Journal of Materials Science: Materials in Medicine 19(5) (2008) 2105-2111.

[27] C. Montero-Ocampo, R. Juarez, A. Salinas Rodriguez, Effect of fcc-hcp phase transformation produced by isothermal aging on the corrosion resistance of a Co-27Cr-5Mo-0.05C alloy, Metallurgical and Materials Transactions A 33(7) (2002) 2229-2235.

[28] K.M. Mantrala, M. Das, V.K. Balla, C.S. Rao, V.V.S. Kesava Rao, Additive Manufacturing of Co-Cr-Mo Alloy: Influence of Heat Treatment on Microstructure, Tribological, and Electrochemical Properties, Frontiers in Mechanical Engineering 1(2) (2015).

[29] C. Valero-Vidal, L. Casabán-Julián, I. Herraiz-Cardona, A. Igual-Muñoz, Influence of carbides and microstructure of CoCrMo alloys on their metallic dissolution resistance, Materials Science and Engineering: C 33 (2013) 4667-4676.

[30] Y. Bedolla-Gil, A. Juarez-Hernandez, A. Perez-Unzueta, E. Garcia-Sanchez, R. Mercado-Solis, M.A.L. Hernandez-Rodriguez, Influence of heat treatments on mechanical properties of a biocompatility alloy ASTM F75, Revista Mexicana De Fisica 55(1) (2009) 1-5.